文章编号：0258-7106（2022）01-0021-14 Doi: 10. 16111/j. 0258-7106. 2022. 01. 002

滇西南云岭锡矿床地质特征与花岗岩锆石 U-Pb 年代学*

萧 珂，孙 祥**，李 强，司晓博，郑 旭，路雷雷，赵泽缘
（中国地质大学 地球科学与资源学院，北京 100083）

摘 要 滇西南是中国重要的锡矿带之一，前人研究主要集中在白垩纪和新生代花岗岩中的锡矿床，而对印支期花岗岩中的锡矿关注较少。云岭锡矿位于保山地块的东缘，矿体主要以脉状产在黑云母二长花岗岩中，发育云英岩化和电气石化蚀变。矿石矿物为锡石，脉石矿物为石英、白云母、电气石、萤石、方解石，以及黄铁矿、毒砂、黄铜矿、闪锌矿等硫化物。根据矿物共生组合以及脉体与蚀变的早晚关系，笔者厘定出4个热液成矿阶段，由早到晚分别为石英-电气石、石英-锡石-白云母-电气石、石英-钾长石±方解石、硫化物±石英阶段。云英岩化黑云母二长花岗岩中的锆石 U-Pb 年龄为(215.6±1.3)Ma，可近似代表云岭锡成矿时代。三叠纪锡成矿作用也发生在昌宁-孟连造山带的临沧岩基及东南亚锡矿带东部，该期成矿作用与古特提斯洋的演化有关。因此，中国滇西南三叠纪锡成矿作用与矿床保存的研究工作还需加强。

关键词 地球化学；花岗岩；锆石 U-Pb 年代学；锡矿；保山地块；滇西南
中图分类号：P618.44 **文献标志码**：A

Geological characteristics and zircon U-Pb geochronology of granite in Yunling tin deposit, southwestern Yunnan

XIAO Ke, SUN Xiang, LI Qiang, SI XiaoBo, ZHENG Xu, LU LeiLei and ZHAO ZeYuan
(School of Earth Science and Mineral Resources, China University of Geosciences, Beijing 100083, China)

Abstract

Southwestern Yunnan is one of important tin metallogenic belts in China. Previous studies mainly focused on tin deposits occurred in Cretaceous and Cenozoic granites, with less attention on tin deposits in Indosinian granites. The Yunling tin deposit is located in the eastern margin of the Baoshan block, ore bodies occur as veins in biotite monzogranite and are associated with greisenization and tourmalinzation. Ore mineral is cassiterite, and gangue minerals comprise quartz, tourmaline, muscovite, fluorite, calcite, pyrite, arsenopyrite, chalcopyrite, and sphalerite. According to mineral assemblages and relationship between hydrothermal veins and alteration, four hydrothermal mineralization stages are identified by author, from early to late including quartz-tourmaline, quartz-cassiterite-muscovite-tourmaline, quartz-K-feldspar ± calcite, and sulfide ± quartz stage. LA-ICP-MS zircon U-Pb isotopic data of biotite monzogranite that was affected by greisenization yielded an age of (215.6±1.3)Ma, which can approximately represent the mineralization age of the Yunling tin deposit. The Triassic tin mineralization also occurred in the Lincang batholith in the Changning-Menglian orogenic belt and in the eastern part of the southeast Asia tin belt, and was related to the evolution of the Paleo-Tethys ocean. Thus, it is necessary to strengthen the studies on ore-forming process and ore preservation of Triassic tin deposits in southwestern Yunnan.

Key words: geochemistry, granite, zircon U-Pb geochronology, tin deposit, Baoshan block, southwestern Yunnan

* 本文得到国家自然科学基金项目(编号: 92162215)资助
第一作者简介 萧 珂，男，1998年生，硕士研究生，矿床学专业。Email: 1803592351@qq.com
** 通讯作者 孙 祥，男，1980年生，教授，从事岩浆-热液成矿作用研究。Email: sunxiang@cugb.edu.cn
收稿日期 2021-11-29；改回日期 2021-12-30。孟秋熠编辑。

锡作为全球性的战略资源,对中国的经济发展和国家安全起到了重要的作用(毛景文等, 2019a)。中国锡矿资源丰富,但由于相关地质工作的投入不充分以及部分矿床开采回收难度大,目前每年所产锡已显明显的颓势,甚至有时需要从国外进口,并不适应中国目前经济发展的节奏(毛景文, 2019b;蒋少涌等, 2020)。考虑到锡具有的重要战略价值,加强其研究十分迫切(侯增谦等, 2020)。

滇西南锡矿带是中国最重要的锡成矿带之一,其向南与东南亚锡成矿带相连,二者同属一个构造-岩浆系统,占据了世界60%以上的锡资源量(施琳等, 1991;卢映祥等, 2009;邓军等, 2010;2011)。滇西南锡矿主要分布于腾冲地块,大量的成岩成矿年代学研究显示锡成矿作用发生在3个时期:第一期是早白垩世(125~120 Ma),代表性矿床为滇滩锡矿(Chen et al., 2014);第二期是晚白垩世(75~68 Ma),代表性矿床为小龙河锡矿(廖世勇等, 2013;Chen et al., 2014;Cao et al., 2016);第三期是古近纪(52~47 Ma),代表性矿床为来利山锡矿(Chen et al., 2014)。近年来,在昌宁-孟连造山带以及保山地块中印支期花岗岩中陆续报道了一系列的锡矿,但是对于这些矿床的矿床地质特征以及成矿时代研究程度较弱(施琳等, 1989;周明山等, 2013;Wang et al., 2014;尹近等, 2019)。云岭锡矿位于保山地块东缘云岭黑云母二长花岗岩体的中部,前人对云岭花岗岩体做了年代学及岩石地球化学方面的工作,但并未关注到云岭锡矿床(聂飞等, 2012)。

本文选择云岭锡矿为研究对象,通过野外调查分析了云岭锡矿的矿体产出特征、矿物组成、成矿阶段及蚀变特征,据此选择云岭锡矿中部V_{10}矿体附近的云英岩化黑云母二长花岗岩进行锆石LA-ICP-MS年代学研究,讨论了成矿时代与区域成矿找矿方向。

1 区域地质特征

滇西南锡矿主要分布在腾冲地块(图1a) ,次为保山地块和昌宁-孟连造山带(图1b) (施琳等, 1989; 1991;卢映祥等, 2009;邓军等, 2010; 2011;Wang et al., 2014)。昌宁-孟连缝合带代表了古特提斯主洋盆,主要经历了晚古生代—中生代古特提斯洋扩张、消减与闭合构造演化过程(Deng et al., 2018;邓军等, 2020)。在昌宁-孟连缝合带中不仅发现古特提斯蛇绿岩(锆石U-Pb年龄为349~331 Ma),也发现了与原特提斯相关蛇绿混杂岩套(锆石U-Pb年龄为473~420 Ma)(王保第等, 2013;Deng et al., 2018)。在昌宁-孟连缝合带东侧出露与之平行的高压变质岩带及巨型复式岩基即临沧岩基(图1b)。临沧岩基呈南北向延伸,长约370 km,宽约50 km,出露面积达7400 km^2,时代主要为261~203 Ma,其形成与古特提斯洋岩石圈东向俯冲及随后的同碰撞和后碰撞过程相关(Hennig et al., 2009;赵枫等, 2018;Deng et al., 2018;Cong et al., 2020)。高压变质带中蓝片岩进变质过程中蓝闪石$^{40}Ar/^{39}Ar$坪年龄(约242 Ma)及勐库退变质榴辉岩锆石U-Pb年龄(约245 Ma)被认为代表古特提斯洋俯冲及闭合事件(Fan et al., 2015;孙载波等, 2018;Wang et al., 2018a)。

腾冲地块位于保山地块西部,二者同属于滇缅泰马地块的北部(图1a) (Metcalfe, 2011)。新特提斯洋向亚欧大陆北向的俯冲以及随后的印度大陆和亚欧大陆的碰撞造成了腾冲地块内部大规模的岩浆活动及相关的矿化作用(Chen et al., 2014;2015;Cao et al., 2016)。腾冲地块花岗岩种类发育较为齐全,早古生代到新生代花岗岩均有分布。早古生代花岗岩(440~520 Ma)仅在高黎贡山两侧有零星出露(Cao et al., 2016)。在梁河地区存在少量的三叠纪—早侏罗世花岗岩(250~190 Ma)(Zhu et al., 2018)。腾冲地块大范围出露的是早白垩世—古近纪花岗岩,可分为早白垩世、晚白垩世、古近纪3个阶段。早白垩世花岗岩以东河岩体为代表,其年龄介于115~131 Ma (Deng et al., 2014;Zhu et al., 2015);晚白垩世花岗岩以古永岩体为代表,其年龄介于70~77 Ma之间(Deng et al., 2014;Cao et al., 2016);古近纪花岗岩以来利山岩体为代表,其年龄介于65~50 Ma之间(Xie et al., 2016;Cao et al., 2017)。这3期花岗岩均发育与之相关的锡矿床,例如滇滩、小龙河、以及来利山锡矿(Chen et al., 2014;Cao et al., 2016)。

保山地块南部与缅甸掸邦地块相连,东部与昌宁-孟连缝合带相接,西部与腾冲地块相邻相连,向北由于怒江与澜沧江断裂汇拢而消失(图1a) (Deng et al., 2014;Metcalfe, 2011;Li et al., 2015;邓军等, 2020;Xu et al., 2021)。保山地块经历特提斯的俯冲及亚欧大陆和印度大陆的碰撞造山过程,岩浆活动频繁。根据前人对保山地块花岗岩年龄的研究,大致可将保山地块的花岗岩分为早古生代、早中生代、晚中生代3期。早古生代花岗岩代表性岩体为平河花岗岩基,其锆石U-Pb年龄为502~466 Ma(Chen et

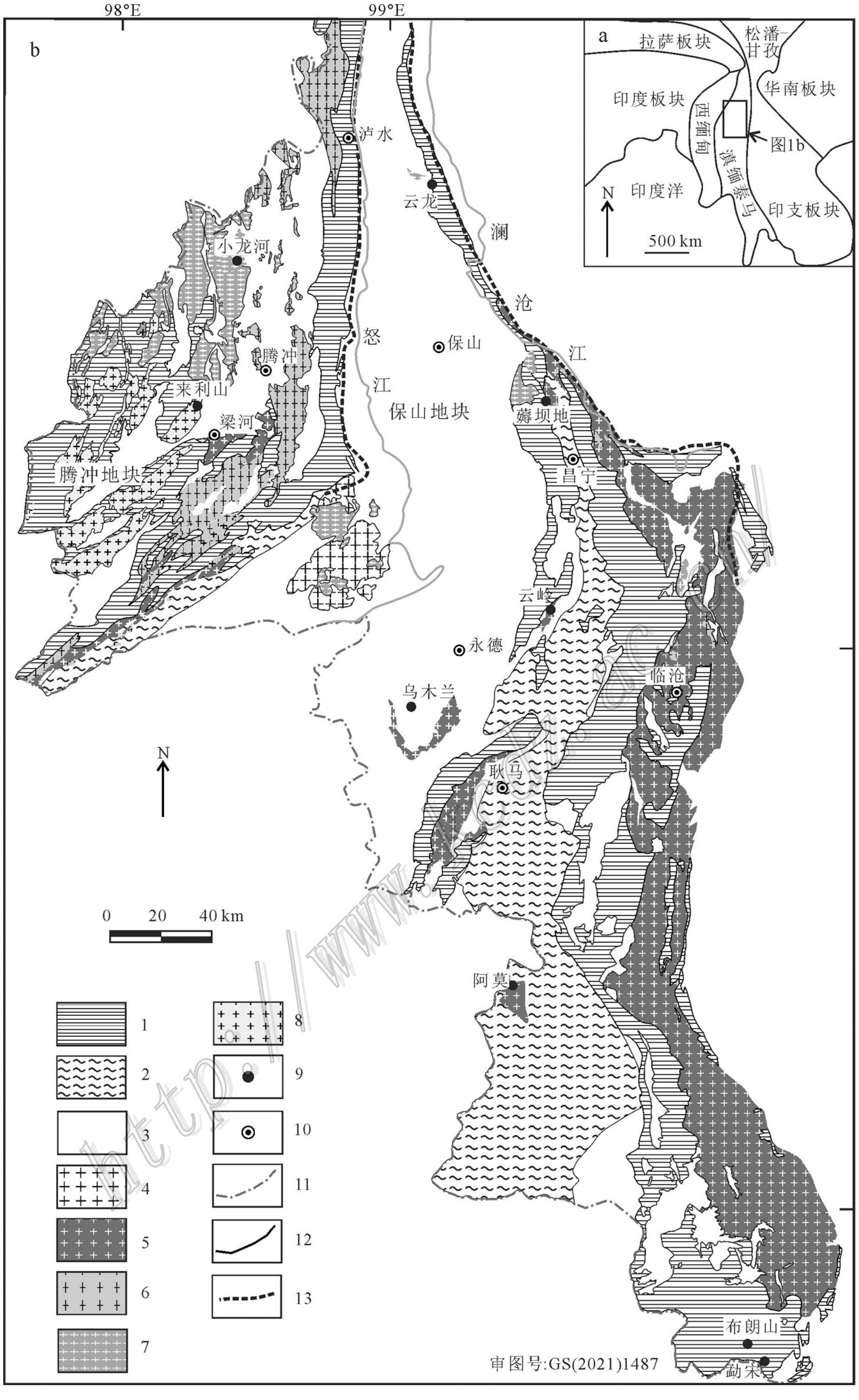

图 1 东南亚构造简图(a,据 Wang et al., 2018)和滇西南花岗岩及锡矿床分布简图(b,据 Deng et al., 2014 修改)

1—前1—前寒武基底;2—缝合带;3—古生代—新生代地层;4—早古生代花岗岩;5—二叠纪—三叠纪花岗岩;6—早白垩世花岗岩;7—晚白垩世花岗岩;8—古近纪花岗岩;9—锡矿床;10—城镇;11—国界线;12—地质界限;13—断层

Fig.1 Tectonic setting of Southeast Asia(a, after Wang et al., 2018) and simplified geologic map showing the distribution of granites and tin deposits in the Baoshan Block, SW Yunnan(b, modified after Deng et al., 2014)

1—Precambrian basement; 2—Suture zone; 3—Paleozoic—Cenozoic strata; 4—Early Paleozoic granites; 5—Permian—Triassic granites; 6—Early Cretaceous granites;7—Late Cretaceous granites; 8—Paleogene granites; 9—Tin deposits; 10—City; 11—Country Border; 12—Geological boundary;13—Fault al., 2007；Liu et al., 2009；董美玲等, 2012；邓军等, 2020；李文昌等, 2010)。早中生代的代表性岩体有木厂花岗岩体、耿马花岗岩体及云岭花岗岩体，其锆石U-Pb年龄分别为240 Ma、232 Ma和231 Ma(聂飞等, 2012；Yang et al., 2019)。晚中生代代表性花岗岩体有志本山、柯街、漕涧等岩体，其锆石U-Pb年龄分别为126 Ma、93 Ma及73 Ma(陶琰等, 2010；廖世勇等, 2013；Deng et al., 2014；禹丽等, 2014；2015)。保山地块岩浆热液型矿床种类较多，包括岩浆Cu-Ni硫化物矿床、矽卡岩型Fe-Cu-Pb-Zn-Au矿床、浅成低温热液型Pb-Zn矿床以及与花岗岩有关的Sn-W矿床 (Jiang et al., 2004；Wang et al., 2018b；Chen et al., 2020；刘金宇, 2020)。这些Sn-W矿床从北向南均有分布，包括云龙、薅坝地、云岭和乌木兰等锡矿床(李光勋, 1986；Jiang et al., 2004；聂飞等, 2012；周明山等, 2013；尹近等, 2019)。

2 矿床地质

云岭锡矿位于云南省永德县亚练乡境内。1981年~1987年，云南省地质局进行1/20万区域调查，提交了《1/20万凤庆幅区域调查报告》。1996年，云南省第四地质大队对云岭一带的锡化探、重砂异常进行了异常查证，在云岭岩体中发现了锡矿。1998年，云南省地勘局第四地质大队经过实地勘查，提交了《云南省永德县亚练乡云岭锡矿扶贫地质勘查报告》，查明锡金属量为7356 t，平均品位约1.5%。

矿区出露地层主要为寒武系储家山组、下泥盆统王家村组、下石炭统平掌组及中侏罗统芦子箐组。储家山组的岩性主要为硅质岩、片岩及砂质板岩；王家村组的岩性主要为页岩及粉砂质灰岩；平掌组岩性主要为玄武岩、安山质玄武岩及凝灰岩；芦子箐组的岩性主要为泥晶灰岩、石英砂岩(图2)。

云岭花岗岩体侵位于中侏罗统芦子箐组以及寒武系储家山组，长约15 km，宽约0.6~3.0 km，出露面积约25 km²。云岭岩体岩性为黑云母二长花岗岩，具有中粗粒花岗结构、片麻状构造。主要造岩矿物为石英(30%)、斜长石(30%)、钾长石(25%)、黑云母(10%)，副矿物主要包括锆石、磷灰石、电气石等。石英多呈他形粒状；斜长石呈半自形板柱状，可见聚片双晶纹，粒径在0.1~0.4 cm左右；钾长石呈半自形-他形板状，部分存在卡式双晶，粒径在0.1~0.3 cm左右；黑云母呈自形-半自形片状，粒径在0.1~0.4 cm左右。

云岭岩体中发育近NS向、NW向及近EW向的断裂。近NS向断裂走向约为330°~14°，倾向35°~80°，沿走向延伸几十米到1000 m左右不等；NW向断裂走向约为105°~145°，倾向15°~55°，沿走向延伸几米到300 m左右不等；近EW向断裂走向约为50°~100°，倾向340°~10°，沿走向延伸从几米到200 m左右不等(周明山等，2013)。

云岭锡矿体主要受构造控制，呈脉状产出，其中主要的矿体为V_{17}、V_{10}、V_{12}，储量占总储量的70%。V_{17}矿体位于矿区中部，呈近SN向脉状产出，沿倾向及走向有舒缓波状变化的趋势，走向延伸约1050 m，其储量占矿区总储量的50%(图2)。V_{17}矿体周围主要发育云英岩化和电气石化(图3a、b，图4a)，其矿物组合为锡石、黄铁矿、黄铜矿与少量毒砂和闪锌矿，以及石英、白云母、电气石(图3b、c，4b、c)。V_{10}及V_{12}矿体位于矿区中部，二者近NW向平行产出，沿走向延伸约320 m左右，矿体周围主要发育电气石化、云英岩化及少量萤石化，其矿物组合为锡石、毒砂、黄铁矿及少量的黄铜矿和闪锌矿，以及石英、电气石、方解石、白云母、萤石、钾长石等(图3c、d，图4d~f)。

根据矿物组合以及脉体相互切穿关系，云岭矿床的脉体从早到晚可被划分为石英-电气石脉、石英-锡石-白云母-电气石脉、石英-钾长石±方解石脉、硫化物±石英脉4种类型。

石英-电气石脉主要呈灰黑色，蜿蜒曲折，在局部出现复合膨大的现象。脉体中主要矿物为石英和电气石。石英为半自形-他形粒状，多呈乳白色。电气石通常为针状集合体，颜色多为淡绿色或无色透明，多出现在脉体与围岩的交界处(图3b，图4h)。与该阶段脉体相关的蚀变为电气石化，主要以电气石团块及电气石细网脉的形式存在(图3b)。

石英-锡石-白云母-电气石脉是主要的锡矿化脉体。矿石矿物主要为锡石，脉石矿物为石英、白云母、电气石及少量绢云母(图3d)。锡石通常以自形粒状或集合体的形态出现，在镜下呈深棕色，部分可见双晶，晶体表面裂隙较多，部分锡石被晚期的硫化物沿裂隙交代(图4d)。白云母通常以自形-半自形的片状存在于锡石周围(图4b)。石英以脉状、团块状形式出现，表面较为干净，与锡石、白云母及电气石共生(图4c)。电气石通常以长柱状或短柱状出现，在镜下呈蓝绿色或棕色，与早阶段电气石明显不同(图4c)。

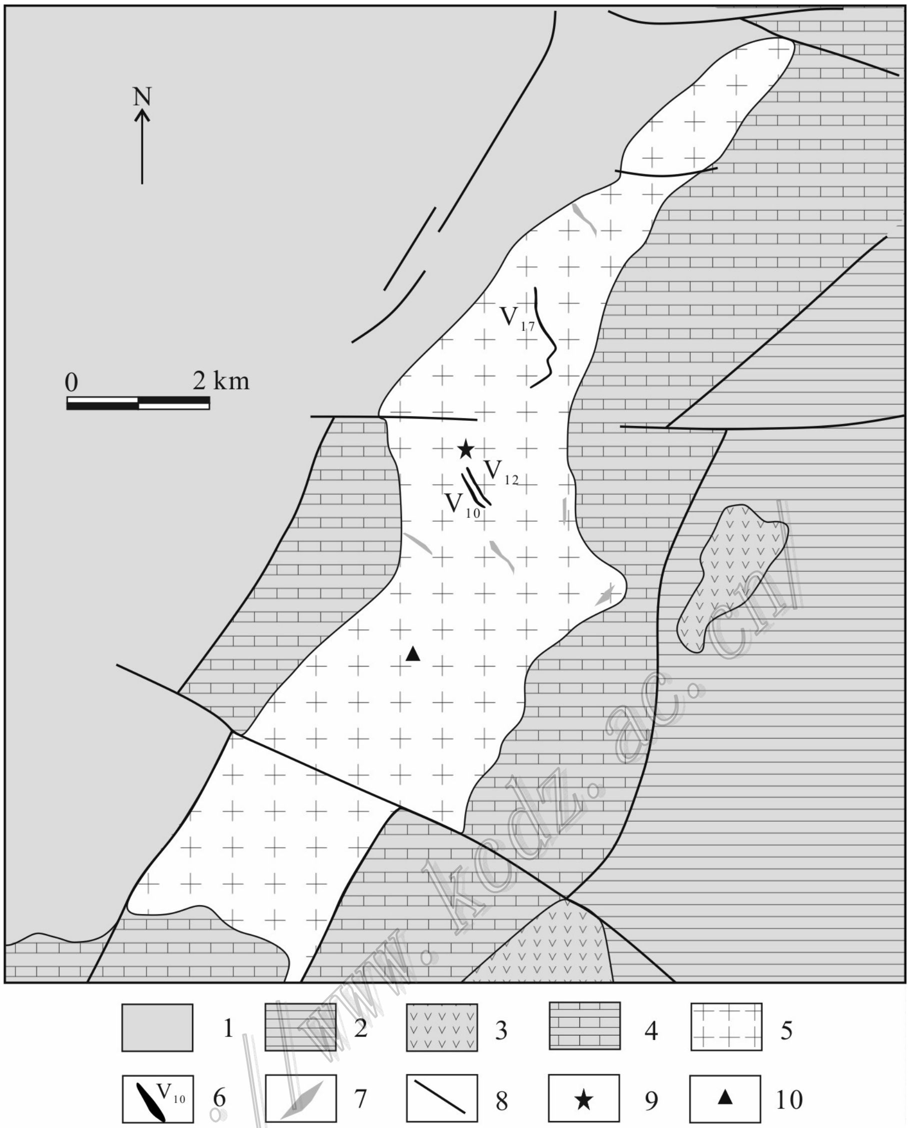

图2　云岭锡矿地质简图(据顾俊生等, 2010；聂飞等, 2012修改)

1—寒武系储家山组硅质岩、片岩、石英砂岩；2—下泥盆统王家村组页岩、粉砂质灰岩；3—下石炭统平掌组玄武岩、安山玄武岩、凝灰岩；4—中侏罗统芦子箐组灰岩、石英砂岩；5—云岭花岗岩；6—矿体及编号；7—石英-电气石脉；8—断层；9—锆石采样点(本文)；10—锆石采样点(前人)

Fig.2　Geologic map of the Yunling tin dposit (modified after Gu et al., 2010；Nie et al., 2012)

1—Siliceous rock, schist and quartz sandstone of Cambrian Chujiashan Formation; 2—Shale and silty limestone of Lower Devonian Wangjiacun Formation; 3—Basalt, Andesitic basalt and tuff of Lower Carboniferous Pingzhang Formation; 4—Limestone and quartz sandstone of Middle Jurassic Luziqing Formation; 5—Yunling granite; 6—Ore body and number; 7—Quartz-tourmaline veins; 8—Fault; 9—Zircon sampling site (this study); 10—Zircon sampling site (previous studies)

石英-钾长石±方解石脉通常以细脉的形式产出，宽约 1~2 mm(图 3c)。该阶段脉体通常交代切割早期石英-电气石及石英-锡石-白云母-电气石脉(图 4e、h)。在该阶段方解石除了在脉体中产出之外，还存在少量方解石交代早期石英-电气石脉(图 4h)。

在最晚阶段发育大量硫化物，以黄铁矿为主，次为毒砂、黄铜矿和闪锌矿等，还出现少量的石英。这些硫化物脉通常切割早期的脉体或锡石(图 3c，图 4d、f)。黄铁矿通常以粒状、团块状及细脉状的形式产出，常与毒砂共生。毒砂多呈银白色，自形-半自形粒状形式产出。在部分黄铁矿中存在毒砂、闪锌矿及黄铜矿包裹体，在闪锌矿中还存在星点状的黄铜矿出溶(图 4d、g)。

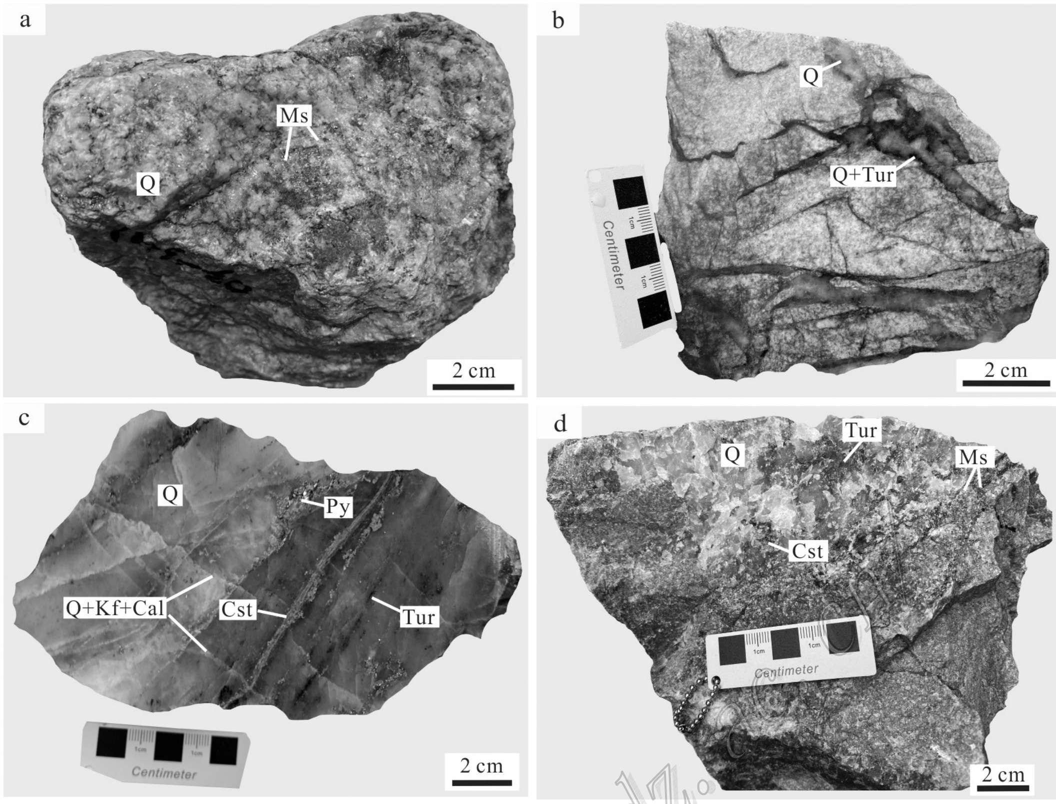

图3 云岭锡矿床花岗岩及矿石照片

a. 云英岩化黑云母二长花岗岩；b. 石英-电气石脉；c. 石英-钾长石-方解石细脉切割锡石脉；d. 石英-锡石-白云母-电气石脉

Cst—锡石；Kf—钾长石；Ms—白云母；Q—石英；Tur—电气石

Fig.3 Photographs of granite and ore from the Yunling tin deposit

a. Biotite monzogranite with greisenization; b. Quartz-tourmaline vein; c. Quartz-k feldspar-calcite vein crosscuts cassiterite vein; d. Quartz-cassiterite-muscovite-tourmaline vein

Cst—Cassiterite; Kf—K-feldspar; Ms—Muscovite; Q—Quartz; Tur—Tourmaline

3 样品描述及测试方法

本次定年所采用的样品为云英岩化黑云母二长花岗岩，采样坐标为：24°10′54″，99°36′03″，采于云岭锡矿 V_{10} 矿体北部。云英岩化黑云母二长花岗岩(YL05-4，图3a)整体呈灰白色，中-细粒结构，块状构造。矿物组成为石英(40%)、长石(25%)、白云母(25%)及少量的方解石。其中，石英呈自形-半自形粒状，粒径0.2~2.0 mm；长石发生白云母化，在局部可见斜长石晶型及聚片双晶纹。副矿物有锆石、磷灰石、电气石等。

锆石分选及制靶工作在北京市首钢地质勘探院完成。具体操作流程为：首先将花岗岩样品粉碎后，经清洗、烘干和筛选，然后采用磁选和浮选法将锆石挑出，最后在双目镜下人工挑选，挑选晶型完整、粒度较大、无明显裂隙和包裹体的锆石进行制靶，并在电镜室内使用日本电子IT-500和DELMIC阴极荧光系统进行锆石阴极发光(CL)拍照，以观察其内部结构。锆石U-Pb年龄在国家地质测试中心进行，激光器波长为193 nm。质谱仪为Thermo Element XR。在剥蚀过程中使用高纯度氦气作为传输气体。在束斑直径为25 μm、频率为10 Hz、能量约为7 mJ的激光下预剥蚀10 s，实际剥蚀40 s，测年所使用标样为锆石91500、610和612，采用Glitter软件处理数据。

4 数据分析

云岭锡矿床的1件云英岩化花岗岩样品(YL05-4)的锆石LA-ICP-MS U-Pb同位素定年结果见表1。该花岗岩中锆石颗粒主要为短柱状、椭圆状，可见四方

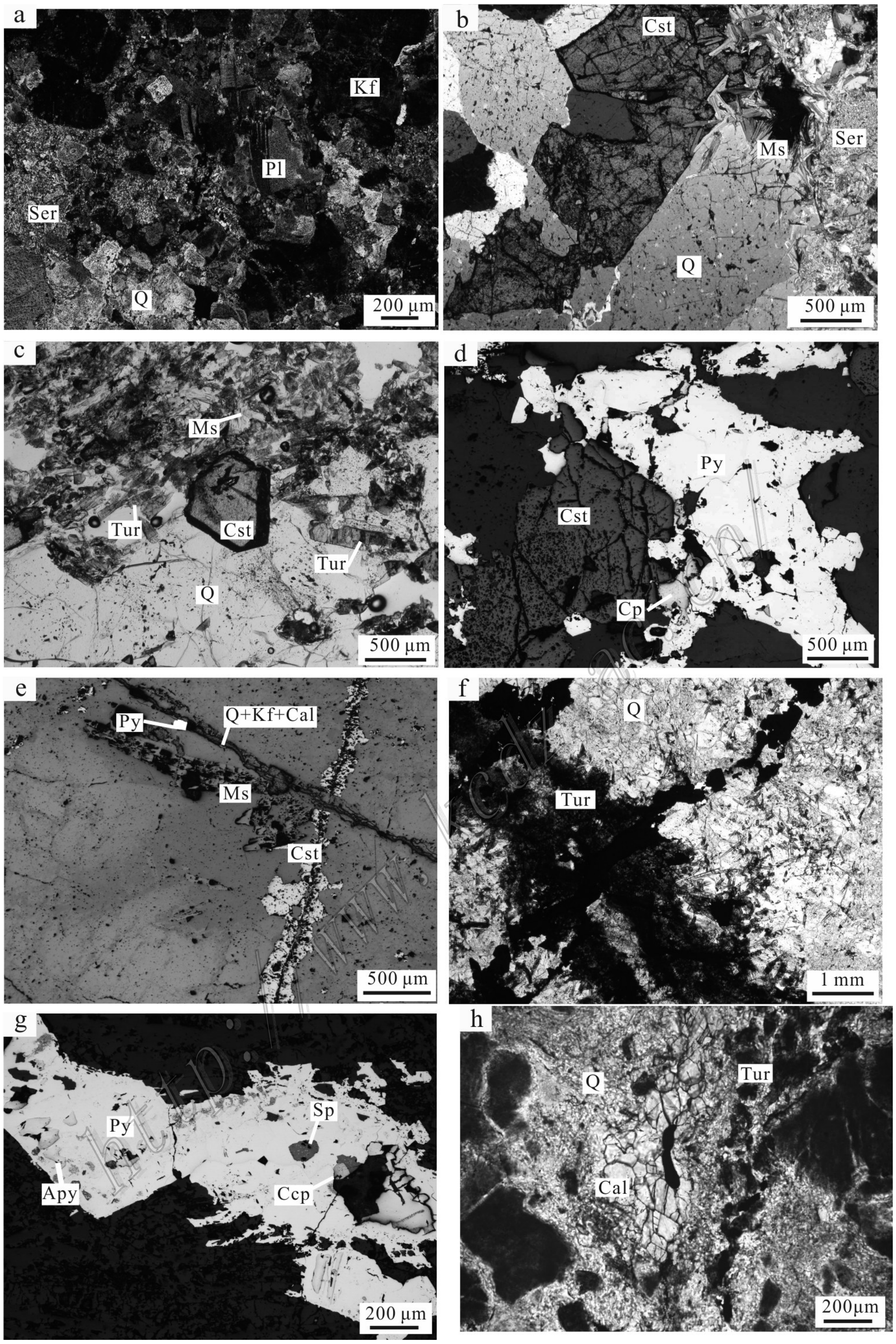

图4　云岭锡矿床花岗岩及矿石镜下照片

a. 云英岩化黑云母二长花岗岩;b. 石英-锡石-白云母脉;c. 自形的锡石与石英、电气石及云母共生;d. 晚期硫化物交代早期锡石;e. 石英-钾长石-方解石脉切穿锡石脉;f. 晚期硫化物切割早期石英-电气石脉;g. 黄铁矿中存在毒砂、黄铜矿及闪锌矿包裹体;h. 早期的石英-电气石脉被晚期方解石及硫化物交代

Apy—毒砂;Cal—方解石;Ccp—黄铜矿; Cst—锡石;Kf—钾长石;Ms—白云母;Pl—斜长石;Py—黄铁矿;Q—石英;Ser—绢云母;Sp—闪锌矿;Tur—电气石

Fig.4　Photomicrographs of granite and ore from the Yunling tin deposit

a. Biotite monzogranite with greisenization; b. Quartz-cassiterite-muscovite vein; c. Euhedral cassiterite is intergrowth with quartz, tourmaline and muscovite; d. Late sulfides cut early cassiterite; e. Quartz-K-feldspar-calcite vein cut cassiterite vein; f. Late sulfides cut early quart-tourmaline vein;

g. Arsenopyrite, chalcopyrite and sphalerite inclusions exist in pyrite; h. Early quartz-tourmaline veins were metasomatized by late calcite and sulfides
Apy—Arsenopyrite; Cal—Calcite; Ccp—Chalcopyrite; Cst—Cassiterite; Kf—K-feldspar; Ms-Muscovite; Pl—Plagioclase; Py—Pyrite; Q—Quartz; Ser—Sericite; Sp—Sphalerite; Tur—Tourmaline

表1 云岭矿床云英岩化黑云母二长花岗岩锆石U-Pb年龄

Table 1 Result of U−Pb dating of Zircons from the Yunling biotite monzogranite that was affected by greisenization

点号	$w(B)/10^{-6}$			Th/U	$^{207}Pb/^{206}Pb$	1σ	$^{207}Pb/^{235}U$	1σ	$^{206}Pb/^{238}U$	1σ	年龄/Ma		
	Pb	Th	U								$^{207}Pb/^{206}Pb$	$^{207}Pb/^{235}U$	$^{206}Pb/^{238}U$
YL05-4_1	19.5	155.4	877.1	0.18	0.0507	0.0025	0.2364	0.0054	0.0338	0.0005	227.9	215.5	214.4
YL05-4_2	19.3	239.6	553.2	0.43	0.0513	0.0019	0.2396	0.0066	0.0339	0.0005	253.2	218.1	214.8
YL05-4_3	22.1	300.2	608.2	0.49	0.0518	0.0017	0.2413	0.0064	0.0338	0.0005	274.9	219.5	214.4
YL05-4_4	10.4	59.9	503.5	0.12	0.0505	0.0016	0.2371	0.0224	0.0341	0.0008	217.0	216.1	216.0
YL05-4_5	24.1	268.5	849.3	0.32	0.0507	0.0014	0.2370	0.0056	0.0339	0.0005	227.6	216.0	214.9
YL05-4_6	36.6	381.2	1310.1	0.29	0.0518	0.0018	0.2425	0.0052	0.0340	0.0005	274.8	220.5	215.4
YL05-4_7	17.6	211.0	587.3	0.36	0.0506	0.0035	0.2374	0.0103	0.0340	0.0006	222.3	216.3	215.7
YL05-4_8	18.1	200.5	580.4	0.35	0.0507	0.0014	0.2364	0.0099	0.0338	0.0006	229.1	215.5	214.3
YL05-4_9	26.4	312.1	801.1	0.39	0.0503	0.0012	0.2360	0.0055	0.0340	0.0005	209.6	215.2	215.7
YL05-4_10	23.5	214.0	942.4	0.23	0.0510	0.0012	0.2388	0.0055	0.0340	0.0005	240.6	217.5	215.3
YL05-4_11	50.6	346.2	336.3	1.03	0.0665	0.0011	0.8451	0.0239	0.0921	0.0015	822.8	622.0	568.2
YL05-4_12	276.5	275.3	2428.4	0.11	0.1370	0.0013	2.6434	0.0477	0.1399	0.0021	2189.7	1312.8	844.3
YL05-4_13	21.7	197.4	934.5	0.21	0.0503	0.0015	0.2369	0.0052	0.0342	0.0005	208.2	215.9	216.6
YL05-4_14	47.3	128.0	157.1	0.81	0.0816	0.0012	2.2629	0.0608	0.2012	0.0033	1235.3	1200.8	1181.7
YL05-4_15	15.8	161.4	548.6	0.29	0.0505	0.0016	0.2426	0.0185	0.0348	0.0008	219.6	220.5	220.6
YL05-4_16	59.0	1088.9	977.0	1.11	0.0497	0.0023	0.2364	0.0139	0.0345	0.0007	180.3	215.5	218.7
YL05-4_17	20.0	82.4	1161.9	0.07	0.0509	0.0013	0.2401	0.0055	0.0342	0.0005	237.0	218.5	216.7
YL05-4_18	16.9	207.2	541.6	0.38	0.0503	0.0010	0.2371	0.0063	0.0342	0.0005	210.4	216.1	216.6
YL05-4_19	5.1	42.4	241.9	0.18	0.0507	0.0011	0.2392	0.0085	0.0342	0.0006	227.4	217.8	216.9
YL05-4_20	14.7	142.2	616.0	0.23	0.0502	0.0014	0.2366	0.0057	0.0342	0.0005	206.3	215.6	216.5
YL05-4_21	7.0	63.0	259.2	0.24	0.0502	0.0016	0.2363	0.0105	0.0342	0.0006	202.9	215.4	216.5
YL05-4_22	36.7	228.1	1826.4	0.12	0.0505	0.0028	0.2374	0.0062	0.0341	0.0005	217.1	216.3	216.2
YL05-4_23	31.3	79.4	191.3	0.41	0.0723	0.0043	1.5908	0.0344	0.1596	0.0025	994.6	966.6	954.3
YL05-4_24	27.3	281.6	972.0	0.29	0.0506	0.0014	0.2365	0.0112	0.0339	0.0006	223.5	215.5	214.8
YL05-4_25	28.4	275.5	1144.9	0.24	0.0521	0.0021	0.2444	0.0053	0.0340	0.0005	291.3	222.0	215.5
YL05-4_26	19.3	218.3	674.6	0.32	0.0507	0.0011	0.2378	0.0064	0.0340	0.0005	225.4	216.6	215.8
YL05-4_27	254.2	690.2	1082.6	0.64	0.0779	0.0019	1.9237	0.0564	0.1790	0.0030	1145.5	1089.4	1061.5
YL05-4_28	22.7	299.5	629.7	0.48	0.0511	0.0021	0.2374	0.0066	0.0337	0.0005	245.0	216.3	213.6
YL05-4_29	28.2	442.5	671.1	0.66	0.0511	0.0014	0.2381	0.0071	0.0338	0.0005	245.3	216.8	214.2
YL05-4_30	19.7	225.6	690.3	0.33	0.0506	0.0063	0.2382	0.0067	0.0341	0.0005	223.3	216.9	216.3
YL05-4_31	23.6	184.9	1057.4	0.17	0.0494	0.0020	0.2353	0.0052	0.0345	0.0005	167.0	214.5	218.9
YL05-4_32	26.6	214.3	1165.9	0.18	0.0511	0.0011	0.2393	0.0053	0.0339	0.0005	247.2	217.9	215.2

双锥晶型,晶面平直,长约100~200 μm。

云岭花岗岩(YL05-4)锆石中的32个测点显示其包含复杂的锆石群。第一组锆石$^{206}Pb/^{238}U$年龄为213.6~220.6 Ma,在CL图像(图5)中,锆石显示较为清晰的环带特征,其$w(U)$介于241.9~1826.4,$w(Th)$介于42.4~1088.9,Th/U比值介于0.18~1.10,表现为典型的

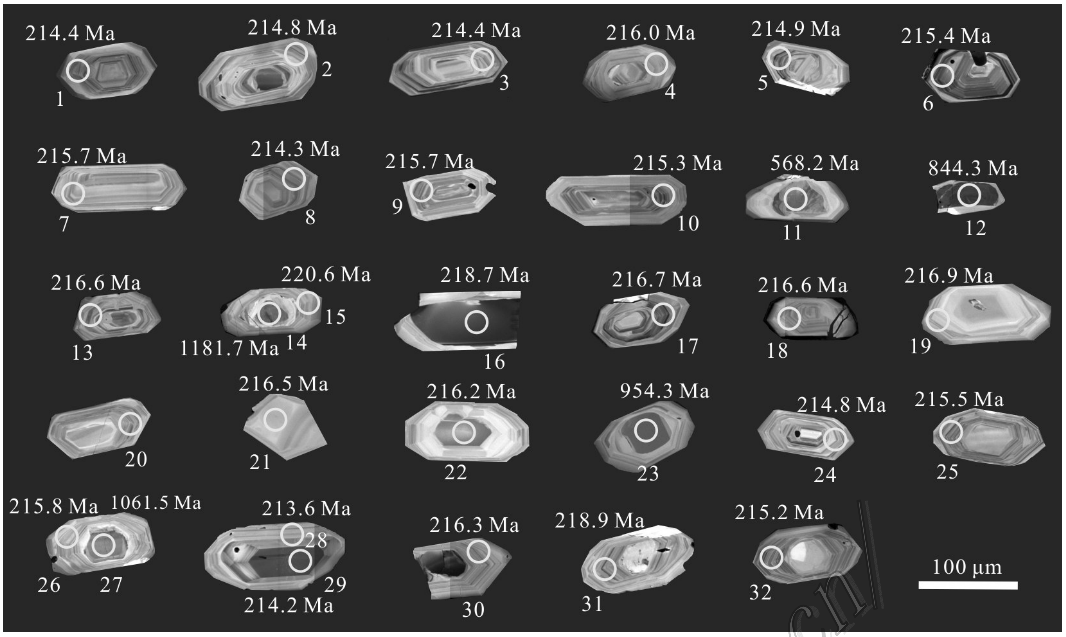

图 5　云岭云英岩化黑云母二长花岗岩锆石阴极发光(CL)图像及年龄

Fig.5　CL image and U-Pb age of zircons from Yunling greisenization biotite monzogranite

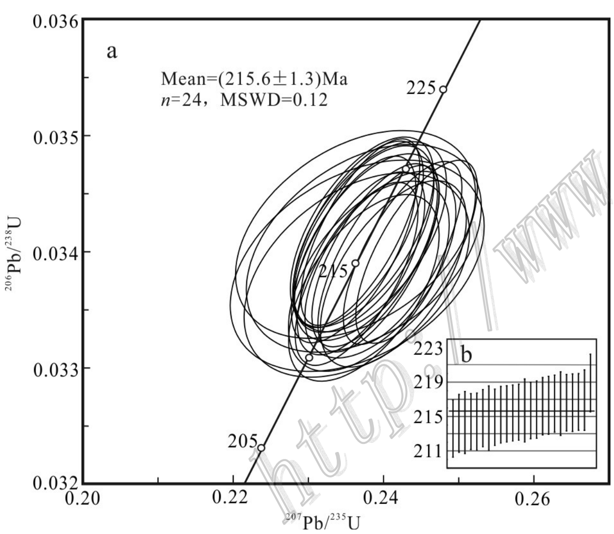

图 6　云岭云英岩化黑云母二长花岗岩锆石 U-Pb 年龄谐和图(a)及加权平均图(b)

Fig.6　Concordia diagram(a) and weighted average diagram (b) of zircon U-Pb age of zircons from Yunling greisenization biotite monzogranite

岩浆锆石特征(Hoskin et al., 2000),锆石大部分投影点在谐和图(图 6a)中,分布于谐和线附近,具有成群分布的特征,总体显示出良好的谐和性,其加权平均年龄(图 6b)为(215.6±1.3)Ma (n=24,MSWD=0.119),该年龄可近似代表云岭锡矿床形成年龄;第二组继承锆石 $^{206}Pb/^{238}U$ 年龄为 568~1181 Ma,该组锆石存在于岩浆锆石的核部,在 CL 下表现为晶型较差,成分较为均一,与岩浆锆石具有明显的明暗区分,该组继承锆石的年龄代表了云岭岩体形成及侵位过程中存在古老基底的贡献。

5　讨　论

5.1　云岭岩体形成时代

聂飞等(2012)对云岭岩体南部黑云母二长花岗岩开展了锆石 U-Pb 年代学与岩石地球化学的研究。云岭黑云母二长花岗岩 $w(SiO_2)$ 约 65%,$w(Al_2O_3)$ 为 13.89%~14.52%,铝饱和指数较高(A/CNK=1.10~1.22),K_2O/Na_2O 比值在 1.42~2.71 之间,$w(CaO)$ 较低(1.35%~2.98%),锆石 Hf 同位素的值为负且变化较大(−26.8~−8.2),这些特征表明云岭黑云母二长花岗岩属过铝质与高钾钙碱性系列,具有壳源 S 型花岗岩特征(聂飞等, 2012)。黑云母二长花岗岩锆石 U-Pb 年龄为(231±3.8)Ma,表明形成于三叠纪(聂飞等, 2012)。

本次研究样品选自云岭岩体中部,位于 V_{12} 矿体北部约 300 m 处,为云英岩化黑云母二长花岗岩样品。通过锆石 U-Pb 定年得出云英岩化黑云母二长花岗岩样品年龄为(215.6±1.3)Ma,可近似代表含锡

花岗岩的侵位年龄。该年龄比聂飞等(2012)获得的锆石U-Pb年龄年轻约15 Ma,可能表明云岭岩体经历了长期的演化。大量的研究也表明,与花岗岩有关的锡矿床多与复式花岗岩体有关,含锡花岗岩通常是晚阶段演化的产物(Chen et al., 2013;Xiong et al., 2020)。

5.2 古特提斯与花岗岩有关的锡成矿作用

西南三江地区是中国特提斯演化过程的重要研究场所,经历了原-古-新特提斯的演化以及印度-欧亚大陆碰撞造山过程,岩浆及成矿作用显著(黄汲清等, 1984;刘增乾等, 1993;钟大赉, 1998;Metcalfe, 2011;Wang et al., 2014;Deng et al., 2014;2018;邓军等, 2020;吴福元等,2020)。

昌宁-孟连造山带内的临沧花岗岩岩性主要为花岗闪长岩与二长花岗岩,侵位时间较长,大致可以分为261~250 Ma之前、250~237 Ma、235~203 Ma三个阶段,分别对应古特提洋的俯冲、同碰撞及后碰撞阶段(Henning et al., 2009;Dong et al., 2013;Deng et al., 2018;邓军等, 2020)。前人通过岩石地球化学的研究发现,临沧花岗岩主要以S型花岗岩为主,含有少量的A型花岗岩(Deng et al., 2018;Cong et al., 2020)。临沧花岗岩南部的布朗山、勐宋一带发育锡矿,含锡花岗岩为二长花岗岩,属于过铝质高钾钙碱性系列,锆石U-Pb年龄为228~216 Ma(施琳等, 1989;Wang et al., 2015)。

值得注意的是,滇西南锡矿带向南与东南亚锡成矿带相连。在马来西亚半岛的东部及西部发育众多锡矿,其形成时代大多数在290~270 Ma和230~210 Ma之间 (Zhang et al., 2021;Yang et al., 2020)。马来西亚晚三叠世的锡矿床大致可分为热液脉型锡矿和矽卡岩型锡矿2种类型(Cao et al., 2020;Yang et al., 2020),矿体多数以锡石-石英脉、含锡的石英-硫化物脉的形式产在花岗岩体中或岩体周围的沉积岩中,矿体的产出多数受构造控制,主要的矿石矿物有锡石、黄铁矿、黄铜矿、毒砂、闪锌矿等,脉石矿物有石英、方解石、绿泥石、绿帘石、白云母(Cao et al., 2020;Du et al., 2019;Yang et al., 2020)。这些特征与云岭锡矿类似。保山地块中除了云岭锡矿,还发育以薅坝地为代表的产于上三叠统石英杂砂岩及碳质页岩中的锡矿,矿体主要受构造控制(施琳等, 1989)。前人在薅坝地矿区外围的癞痢头山花岗岩开展了年代学研究,获得了锆石U-Pb年龄为(231.5±3.6)Ma(聂飞等, 2012;尹近等, 2019),但是否与成矿相关尚不清楚。

相比于东南亚锡矿床的规模及数量来看,中国滇西南与古特提斯演化有关的花岗中锡矿规模目前已知的相对较弱,亟待加强成矿作用与矿床保存等方面的研究。

6 结 论

(1)云岭锡矿矿体主要以脉状产在黑云母二长花岗岩中,成矿阶段可分为石英-电气石、石英-锡石-白云母-电气石、石英-钾长石±方解石以及硫化物±石英4个阶段。

(2)云岭锡矿化与云英岩化关系密切。锆石U-Pb年代学研究显示云英岩化黑云母二长花岗岩的年龄为(215.6±1.3)Ma,可近似代表云岭锡矿的形成时代。

(3)滇西南东部三叠纪花岗岩中的锡矿化可与马来西亚230~210 Ma的锡成矿类比,但目前已知的成矿规模相对较小,亟待加强成矿作用与矿床保存等方面的研究。

致 谢 野外工作得到了中国地质大学(北京)李强硕士、司晓博、郑旭博士的协助;实验工作得到了国家地质测试中心周利敏和孙冬阳老师的大力协助;在成文过程中与中国地质大学(北京)路雷雷硕士进行了有益的讨论;同时审稿专家对于本文的修改提出了众多富有建设性的意见,在此一并表示衷心的感谢!

References

Cao H W, Zou H, Zhang Y H, Zhang S T, Zheng L and Zhang L K. 2016. Late Cretaceous magmatism and related metallogeny in the Tengchong area: Evidence from geochronological, isotopic and geochemical data from the Xiaolonghe Sn deposit, western Yunnan, China[J]. Ore Geology Reviews, 78: 196-212.

Cao H W, Pei Q M, Zhang S T, Zhang L K, Tang L, Lin J Z and Zheng L. 2017. Geology, geochemistry and genesis of the Eocene Lailishan Sn deposit in the Sanjiang region, SW China[J]. Journal of Asian Earth Sciences, 137: 220-240.

Cao J Y, Yang X Y, Du G F and Li H. 2020. Genesis and tectonic setting of the Malaysian Waterfall granites and tin deposit: Constraints from LA-ICP(MC)-MS zircon U-Pb and cassiterite dating and Sr-Nd-Hf isotopes[J]. Ore Geology Reviews, 118: 103336.

Chen F C, Deng J, Wang Q F, Hui Z G, Jan M T, Li G J and Gu Y W. 2020. LA-ICP-MS trace element analysis of magnetite and pyrite from the Hetaoping Fe-Zn-Pb skarn deposit in Baoshan block, SW China: Implications for ore-forming processes[J]. Ore Geology Reviews, 117: 103309.

Chen F K, Li X H, Wang X L, Li Q L and Siebel W. 2007. Zircon age and Nd-Hf isotopic composition of the Yunnan Tethyan belt, southwestern China[J]. International Journal of Earth Sciences, 96 (6): 1179-1194.

Chen J, Wang R C, Zhu J C, Lu J J and Ma D S. 2013. Multiple-aged granitoids and related tungsten-tin mineralization in the Nanling range, South China[J]. Science China-Earth Science, 56: 385-413.

Chen X C, Hu R Z, Bi X W, Li H M, Lan J B, Zhao C H and Zhu J J. 2014. Cassiterite LA-MC-ICP-MS U/Pb and muscovite $^{40}Ar/^{39}Ar$ dating of tin deposits in the Tengchong-Lianghe tin district, NW Yunnan, China[J]. Mineralium Deposita, 49(7): 843-860.

Chen X C, Hu R Z, Bi X W, Zhong H, Lan J B, Zhao C H and Zhu J J. 2015. Petrogenesis of metaluminous A-type granitoids in the Tengchong-Lianghe tin belt of southwestern China: Evidences from zircon U-Pb ages and Hf-O isotopes, and whole-rock Sr-Nd isotopes[J]. Lithos, 212: 93-110.

Cong F, Wu F Y, Li W C, Mou C L, Huang X M, Wang B D, Hu F Y and Peng Z M. 2020. Origin of the Triassic Lincang granites in the southeastern Tibetan Plateau: Crystallization from crystal mush[J]. Lithos, 360: 105452.

Deng J, Hou Z Q, Mo X X, Yang L Q, Wang Q F and Wang C M. 2010. Superimposed orogenesis and metallogenesis in Sanjiang Tethys[J]. Minerals Deposits, 29(1): 37-42(in Chinese with English abstract).

Deng J, Yang L Q and Wang C M. 2011. Research advances of superimposed orogenesis and metallogenesis in the Sanjiang Tethys[J]. Acta Petrologica Sinica, 27(9): 2501-2509(in Chinese with English abstract).

Deng J, Wang Q F, Li G J, Li C S and Wang C M. 2014. Tethys tectonic evolution and its bearing on the distribution of important mineral deposits in the Sanjiang region, SW China[J]. Gondwana Research, 26(2): 419-437.

Deng J, Wang C M, Zi J W, Xia R and Li Q. 2018. Constraining subduction-collision processes of the Paleo-Tethys along the Changning-Menglian Suture: New zircon U-Pb ages and Sr-Nd-Pb-Hf-O isotopes of the Lincang Batholith[J]. Gondwana Research, 62: 75-92.

Deng J, Wang Q F, Cheng F C, Li G J, Yang L Q, Wang C M, Zhang J, Sun X, Shu Q H, He W Y, Gao X, Gao L, Liu X F, Zheng Y C, Qiu K F, Xue S C and Xu J H. 2020. Further discussion on the Sanjiang Tethyan composite metallogenic system[J]. Earth Science Frontiers, 27(2): 107-136(in Chinese with English abstract).

Dong M L, Dong G C, Mo X X, Zhu D C, Nie F, Xie X F, Wang X and Hu Z C. 2012. Geochronology and geochemistry of the Early Palaeozoic granitoids in Baoshan block, western Yunnan and their implications[J]. Acta Petrologica Sinica, 28(5): 1453-1464(in Chinese with English abstract).

Dong G C, Mo X X, Zhao Z D, Zhu D C, Goodman R C, Kong H L and Wang S. 2013. Zircon U-Pb dating and the petrological and geochemical constraints on Lincang granite in western Yunnan, China: Implications for the closure of the Paleo-Tethys Ocean[J]. Journal of Asian Earth Sciences, 62: 282-294.

Du G F, Yang X Y, Cao J Y and Abdul A J. 2019. Genesis and timing of the Sungai Lembing tin deposit in Pahang, East Malaysia: Constraints from LA-ICP-MS zircon and cassiterite U-Pb dating, geochemical compositions and Sr-Nd-Hf isotopes[J]. Ore Geology Reviews, 119: 103364.

Fan W M, Wang Y J, Zhang Y H, Zhang Y Z, Jourdan F, Zi J W and Liu H C. 2015. Paleotethyan subduction process revealed from Triassic blueschists in the Lancang tectonic belt of Southwest China[J]. Tectonophysics, 662(1): 95-108.

Gu J S, Wang Y and Zhai Y X. 2010. Resources and reserves verification report of Yunling tin mine, Yongde County, Yunnan Province[R]. Yunnan Institute of Nuclear Geological Survey(in Chinese).

Hennig D, Lehmann B, Frei D, Belyatsky B, Zhao X F, Cabral A R, Zeng P S, Zhou M F and Schmidt K. 2009. Early Permian seafloor to continental arc magmatism in the eastern Paleo-Tethys: U-Pb age and Nd-Sr isotope data from the southern Lancangjiang zone, Yunnan, China[J]. Lithos, 113(3-4): 408-422.

Hoskin P W and Black L P. 2000. Metamorphic zircon formation by solid-state recrystallization of protolith igneous zircon[J]. Journal of Metamorphic Geology, 18: 423-439.

Hou Z Q, Chen J and Zhai M G. 2020. Current status and frontiers of research on critical mineral resources[J]. Chinese Science Bulletin, 65(33): 3651-3652(in Chinese with English abstract).

Huang J Q, Chen G M and Chen B W. 1984. Preliminary analysis of the tethyshimalaya tectonic domain[J]. Acta Geologica Sinica, 58 (1): 1-17(in Chinese with English abstract).

Jiang S Y, Yu J M and Lu J J. 2004. Trace and rare-earth element geochemistry in tourmaline and cassiterite from the Yunlong tin deposit, Yunnan, China: Implication for migmatitic-hydrothermal fluid evolution and ore genesis[J]. Chemical Geology, 209: 193-213.

Jiang S Y, Zhao K D, Jiang H, Su H M, Xiong S F, Xiong Y Q, Xu Y M, Zhang W and Zhu L Y. 2020. Spatiotemporal distribution, geological characteristics and metallogenic mechanism of tungsten and tin deposits in China: An overview[J]. Chinese Science Bulletin, 65: 3730-345(in Chinese with English abstract).

Li W C, Pan G T, Hou Z Q and Mo X X. 2010. Archipelagic-Basin, forming collision theory and prospecting techniques along the Nujiang-Lancangjiang-Jinshajiang area in southwestern China[M]. Beijing: Geol. Pub. House. 201p(in Chinese).

Liao S Y, Wang D B, Tang Y, Yin F G, Sun Z M and Sun J. 2013. LA-ICP-MS U-Pb age of two-mica granite in the Yunlong tin-tungsten metallogenic belt in Three River region and its geological implications[J]. Acta Petrologica et Mineralgica, 32(4): 450-462(in Chinese with English abstract).

Li G J, Wang Q F, Huang Y H, Chen F C and Dong P. 2015. Discovery of Hadean-Mesoarchean crustal materials in the northern Sibumasu block and its significance for Gondwana reconstruction[J]. Precambrian Research, 271: 118-137.

Li G X. 1986. The ore field structure and deposit features of tin deposits at Tiechang, Yunlong county[J]. Yunnan Geology, 2: 127-136(in Chinese with English abstract).

Liu J Y. 2020. The study of late paleozoic basaltic magmatism and associated nickel copper metallogeny in the Baoshan block, Sanjiang Tethys Belt, SW China[D]. Supervisor: Deng J. (Beijing) China University of Geosciences. 168p(in Chinese with English abstract).

Liu S, Hu R Z, Gao S, Feng C X, Huang Z L, Lai S C, Yuan H L, Liu X M, Coulson I M, Feng G Y and Wang T. 2009. U-Pb zircon, geochemical and Sr-Nd-Hf isotopic constraints on the age and origin of Early Palaeozoic I-type granite from the Tengchong-Baoshan block, western Yunnan Province, SW China[J]. Journal of Asian Earth Sciences, 36(2-3): 168-182.

Liu Z Q, Li X Z and Ye Q T. 1993. Division of tectono-magmatic zones and the distribution of deposits in the Sanjiang area[M]. Beijing: Geological Publishing House. 246p(in Chinese).

Lu Y X, Liu H G, Huang J N, Zhang H Y and Chen Y Q. 2009. Preliminary division of the metallogenetic belts in the Central South Peninsula of southeast Asia and their regional ore-forming characteristics[J]. Geological Bulletin of China, 28 (2-3): 314-325(in Chinese with English abstract).

Mao J W, Yuan S D, Xie G Q, Song S W, Zhou Q, Gao Y B, Liu X, Fu X F, Cao J, Zeng Z L, Li G T and Fan X Y. 2019a. New advances on metallogenic studies and exploration on critical minerals of China in 21st Century[J]. Mineral Deposits, 38(5): 935-969(in Chinese with English abstract).

Mao J W, Yang Z X, Xie G Q, Yuan S D and Zhou Z H. 2019b. Critical minerals: International trends and thinking[J]. Mineral Deposits, 38(4): 689-698(in Chinese with English abstract).

Metcalfe I. 2011. Tectonic framework and Phanerozoic evolution of Sundaland[J]. Gondwana Research, 19: 3-21.

Nie F, Dong G C, Mo X X, Zhu D C, Dong M L and Wang X. 2012. Geochemistry, zircon U-Pb chronology of the Triassic granites in the Changning-Menglian suture zone and their implications[J]. Acta Petrologica Sinica, 28(5): 1465-1476(in Chinese with English abstract).

Shi L, Chen J C, Wu S L and Peng X J. 1989. Minerogenetic patterns of the tin belt in western in Yunnan[M]. Beijing: Geological Publishing House. 296p(in Chinese).

Shi L, Tang L D, Zhao M and Zhang W L. 1991. Typea of primary tin ore deposit and metallogenic mechanism in Tengchon-Lianghe area[J]. Yunnan Geology, 10(3): 290-322(in Chinese with English abstract).

Sun Z B, Li J, Zhou K, Zeng W T, Wu J L, Hu S B, Liu G C and Zhao J T. 2018. Zircon U-Pb age and geological significance of retrograded eclogites from Mengku area in western Yunnan Province[J]. Geological Bulletin of China, 37(11): 2032-2043(in Chinese with English abstract).

Tao Y, Hu R Z, Zhu F L, Ma Y S, Ye L and Cheng Z T. 2010. Ore-forming age and the geodynamic background of the Hetaoping lead-zinc deposit in Baoshan, Yunnan[J]. Acta Petrologica Sinica, 26(6): 1760-1772(in Chinese with English abstract).

Wang B D, Wang L Q, Pan G T, Yin F G, Wang D B and Tang Y. 2013. U-Pb zircon dating of Early Paleozoic gabbro from the Nantinghe ophiolite in the Changning-Menglian suture zone and its geological implication[J]. Chinese Science Bulletin, 58(4): 344-354(in Chinese with English abstract).

Wang C M, Deng J, Carranza E J and Santosh M. 2014. Tin metallogenesis associated with granitoids in the southwestern Sanjiang Tethyan Domain: Nature, deposit types, and tectonic setting[J]. Gondwana Research, 26(2): 576-593.

Wang C M, Deng J, Santosh M, Lu Y J, McCuaig T C, Carranza E J and Wang Q. 2015. Age and origin of the Bulangshan and Mengsong granitoids and their significance for post-collisional tectonics in the Changning Menglian Paleo-Tethys orogen[J]. Journal of Asian Earth Sciences, 113(2): 656-676.

Wang H N, Liu F L, Li J, Sun Z B, Ji L, Tian Z H, Liu L S and Santosh M. 2018a. Petrology, geochemistry and *P-T-t* path of lawsonite-bearing retrograded eclogites in the Changning-Menglian orogenic belt, southeast Tibetan Plateau[J]. Journal of Metamorphic Geology, 37(4): 439-478.

Wang Q F, Deng J, Li G J, Liu J Y, Li C S and Ripley E M. 2018b. Geochronological, petrological, and geochemical studies of the Daxueshan magmatic Ni-Cu sulfide deposit in the Tethyan Orogenic Belt, southwest China[J]. Econ. Geol., 113(6): 1307-1332.

Wang Y J, Qian X, Cawood P A, Liu H C, Feng Q L, Zhao G C, Zhang Y H, He H Y and Zhang P Z. 2018. Closure of the East Paleotethyan ocean and amalgamation of the eastern Cimmerian and southeast Asia continental fragments[J]. Earth Since Reviews, 186: 195-230.

Wu F Y, Wan B, Zhao L, Xiao W J and Zhu R X. 2020. Tethyan geodynamics[J]. Acta Petrologica Sinica, 36(6): 1627-1674(in Chinese with English abstract).

Xie J C, Zhu D C, Dong G C, Zhao Z D, Wang Q and Mo X X. 2016. Linking the Tengchong Terrane in SW Yunnan with the Lhasa Terrane in southern Tibet through magmatic correlation[J]. Gondwana Research, 39: 217-229.

Xiong Y Q, Shao Y J, Cheng Y B and Jiang S Y. 2020. Discrete jurassic and cretaceous mineralization events at the Xiangdong W(-Sn) deposit, Nanling Range, South China[J]. Econ. Geol., 115(2): 383-

413.

Xu R, Chen W, Deng M G, Li W C, Chen F C, Lai C K, Sha J Z, Jia Z and Liu W. 2021. Geology and C-O-S-Pb isotopes of the Fangyangshan Cu-Pb-Zn deposit in the Baoshan block (SW China): Implications for metal source and ore genesis[J]. Ore Geology Reviews, 103992.

Yang F C, Li W C, Liu X L, Wang S S, Yang Y K, Gu Y W and Luo Y. 2019. Zircon U-Pb ages of the Muchang alkali granites in Zhenkang Block, western Yunnan: Implication for the time limit on tectono-magmatic activities[J]. Acta Geologica Sinica (English edition), 93(4): 1152-1153.

Yang J H, Zhou M F, Hu R Z, Zhong H, Williams J A, Liu L, Zhang X C and Wei Mao. 2020. Granite-related tin metallogenic events and key controlling factors in peninsular Malaysia, southeast Asia: New insights from cassiterite U-Pb dating and zircon geochemistry[J]. Econ. Geol., 115(3):581-601.

Yin J, Shi D Q and Long X Y. 2019. Characteristics of granite in Haobadi tin deposit, Changning County, Yunnan Province[J]. Resources Environment and Engineering, 33(1): 22-26(in Chinese with English abstract).

Yu L, Li G J, Wang Q F and Liu X F. 2014. Petrogenesis and tectonic significance of the Late Cretaceous magmatism in the northern part of the Baoshan block: Constraints from bulk geochemistry, zircon U-Pb geochronology and Hf isotopic compositions[J]. Acta Petrologica Sinica, 30(9): 2709-2724(in Chinese with English abstract).

Yu L, Wang Q F, Li G J and Gao L. 2015. Geochemistry, zircon U-Pb geochronology of granitic pegmatites from Caojian area in the northern Baoshan block, and their geological significance[J]. Acta Petrologica Sinica, 31(11): 3281-3296(in Chinese with English abstract).

Zhang Q, Zhao K D, Li W Q, Palmer M R, Jiang S Y, Jiang H, Zhang W, Zhang D and Hussain A. 2021. Timing and tectonic setting of tin mineralization in southern Myanmar: Constraints from cassiterite and wolframite U-Pb ages[J]. Mineralium Deposita. https://doi.org/10.1007/s00126-021-01083-y.

Zhao F, Li G J, Zhang P F, Wang C B, Sun Z B and Tang X. 2018. Petrogenesis and tectonic implications of the Lincang batholith in the Sanjiang, southwest China: Constraints by geochemistry, zircon U-Pb chronology and Hf isotope[J]. Acta Petrologica Sinica, 34(5): 1397-1412(in Chinese with English abstract).

Zhong D B. 1998. Paleoteyan orogenic belt in western Yunnan and Sichuang[M]. Beijing: Science Press. 231p(in Chinese).

Zhou M S, Zhang X Y and Chen L J. 2013. Ore-controlling Rules of Yunling metallogenic belt in Yunan Province[J]. Resources Tribune, 11: 18-21(in Chinese with English abstract).

Zhu R Z, Lai S C, Qin J F and Zhao S W. 2015. Early-Cretaceous highly fractionated I-type granites from the northern Tengchong block, western Yunnan, SW China: Petrogenesis and tectonic implications[J]. Journal of Asian Earth Sciences, 100(15): 145-163.

Zhu R Z, Lai S C Qin J F and Zhao S W. 2018. Petrogenesis of late Paleozoic-to-early Mesozoic granitoids and metagabbroic rocks of the Tengchong Block, SW China: Implications for the evolution of the eastern Paleo-Tethys[J]. International Journal of Earth Sciences, 107 (2): 431-457.

附中文参考文献

邓军，侯增谦，莫宣学，杨立强，王庆飞，王长明. 2010. 三江特提斯复合造山与成矿作用[J]. 矿床地质, 29(1): 37-42.

邓军，杨立强，王长明. 2011. 三江特提斯复合造山与成矿作用研究进展[J]. 岩石学报, 27(9): 2501-2509.

邓军，王庆飞，陈福川，李龚健，杨立强，王长明，张静，孙祥，舒启海，和文言，高雪，高亮，刘学飞，郑远川，邱昆峰，薛胜超，徐佳豪. 2020. 再论三江特提斯复合成矿系统[J]. 地学前缘, 27(2): 107-136.

董美玲，董国臣，莫宣学，朱弟成，聂飞，谢许峰，王霞，胡兆初. 2012. 滇西保山地块早古生代花岗岩类的年代学、地球化学及意义[J]. 岩石学报, 28(5): 1453-1464.

黄汲清，陈国铭，陈炳蔚. 1984. 特提斯喜马拉雅构造域初步分析[J]. 地质学报, 58(1): 1-17.

顾俊生，王玉忠，翟映祥. 2010. 云南省永德县云岭锡矿核查矿区资源储量核查报告[R]. 云南省核工业地质调查院.

侯增谦，陈骏，翟明国. 2020. 战略性关键矿产研究现状与科学前沿[J]. 科学通报, 65(33):3651-3652.

蒋少涌，赵葵东，姜海，苏慧敏，熊索菲，熊伊曲，徐耀明，章伟，朱律运. 2020. 中国钨锡矿床时空分布规律、地质特征与成矿机制研究进展[J]. 科学通报, 65: 3730-345.

李光勋. 1986. 云龙铁厂锡矿矿田构造和矿床特征[J]. 云南地质, 2: 127-136.

李文昌，潘桂棠，侯增谦，莫宣学. 2010. 西南"三江"多岛弧盆碰撞造山成矿理论与勘查技术[M]. 北京：地质出版社. 201 页.

廖世勇，王冬兵，唐渊，尹福光，孙志明，孙洁. 2013."三江"云龙锡(钨)成矿带晚白垩世二云母花岗岩 LA-ICP-MS 锆石 U-Pb 定年及其地质意义[J]. 岩石矿物学杂志, 32(4): 450-462.

刘增乾，李兴振，叶庆同. 1993. 三江地区构造岩浆带的划分与矿产分布规律[M]. 北京: 地质出版社. 246 页.

刘金宇. 2020. 西南三江特提斯保山地块晚古生代玄武质岩浆作用与镍-铜成矿研究[D]. 导师:邓军. 北京: 中国地质大学.

卢映祥，刘洪光，黄静宁，张宏远，陈永清. 2009. 东南亚中南半岛成矿带初步划分与区域成矿特征[J]. 地质通报, 28 (2-3): 314-325.

施琳，陈吉琛，吴上龙，彭新阶. 1989. 滇西锡矿带成矿规律[M]. 北京：地质出版社. 296 页.

施琳，唐良栋，赵珉，张为鹏. 1991. 腾冲-梁河地区原生锡矿床类型及成矿机理[J]. 云南地质, 10(3): 290-322.

孙载波，李静，周坤，曾文涛，吴嘉林，胡绍斌，刘桂春，赵江泰. 2018. 滇西勐库地区退变质榴辉岩锆石 U-Pb 年龄及其地质意义[J]. 地质通报, 37(11): 2032-2043.

毛景文，袁顺达，谢桂青，宋世伟，周琦，高永宝，刘翔，付小方，曹晶，

曾载淋,李通国,樊锡银. 2019a. 21世纪以来中国关键金属矿产找矿勘查与研究新进展[J]. 矿床地质, 38(5): 935-969.

毛景文,杨宗喜,谢桂青,袁顺达,周振华. 2019b. 关键矿产——国际动向与思考[J]. 矿床地质, 38(4): 689-698.

聂飞,董国臣,莫宣学,朱弟成,董美玲,王霞. 2012. 滇西昌宁-孟连带三叠纪花岗岩地球化学、年代学及其意义[J]. 岩石学报, 28(5): 1465-1476.

陶琰,胡瑞忠,朱飞霖,马言胜,叶霖,程增涛. 2010. 云南保山核桃坪铅锌矿成矿年龄及动力学背景分析[J]. 岩石学报, 26(6): 1760-1772.

王保弟,王立全,潘桂棠,尹福光,王冬兵,唐渊. 2013. 昌宁-孟连结合带南汀河早古生代辉长岩锆石年代学及地质意义[J]. 科学通报, 58(4): 344-354.

吴福元,万博,赵亮,肖文交,朱日祥. 2020. 特提斯地球动力学[J]. 岩石学报, 36(6): 1627-1674.

尹近,石德强,龙兴跃. 2019. 云南昌宁薅坝地锡矿花岗岩特征[J]. 资源环境与工程, 33(1): 22-26.

禹丽,李龚健,王庆飞,刘学飞. 2014. 保山地块北部晚白垩世岩浆岩成因及其构造指示:全岩地球化学、锆石U-Pb年代学和Hf同位素制约[J]. 岩石学报, 30(9): 2709-2724.

禹丽,王庆飞,李龚健,高磊. 2015. 保山地块漕涧花岗伟晶岩地球化学、锆石U-Pb年代学及其地质意义[J]. 岩石学报, 31(11): 3281-3296.

赵枫,李龚健,张鹏飞,王传斌,孙载波,唐鑫. 2018. 西南三江临沧花岗岩基成因与构造启示: 元素地球化学、锆石 U-Pb 年代学及 Hf 同位素约束[J]. 岩石学报, 34(5): 1397-1412.

钟大赉. 1998. 滇川西部古特提斯造山带[M]. 北京: 科学出版社. 231页.

周明山,张晓永,陈丽娟. 2013. 云南省云岭成矿带控矿规律研究[J]. 资源导刊, 11: 18-21.